Performance Analysis Of Hyperspectral Data Classification Based On Hybrid Neural Network Approach

Rajashree Gadhave, R. R. Sedamkar, Sujata Alegavi
Research Scholar, Thakur College of Engineering and Technology, University of Mumbai, India
Professor & HoD (PhD programs), Thakur College of Engineering and Technology, University of Mumbai, India
Assistant Professor, Thakur college of Engineering and Technology, University of Mumbai, India.

Abstract:
Hyperspectral Image (HSI) data classification is a challenging task in remote sensing data analysis, which has been applied in many domains for better identification and inspection of the earth surface by extracting spectral and spatial information. Recent advances in neural networks have made great progress in the HSI classification. However, many traditional methods are based on handcrafted features, which brings difficulties for multi-classification tasks due to spectral intra-class heterogeneity, similarity of inter-class and higher model complexity. Consequently, conventional classifiers are not feasible to extract distinctive features. In order to improve the classification, this paper presented a hybrid neural network approach with pretrained DNN model with ANN based method. The performance of proposed classifiers is compared and found to be effective, Overall improvement in a classification performance is 4.6% in comparison with existing methods. Though, this model could be applied and validated on geological mapping and urban investigation in terms of live hyperspectral image dataset.
Keywords: convolutional neural networks; feature fusion; high spatial resolution; multilayer feature maps; hyperspectral band and image
DOI: 10.24297/j.cims.2023.5.3

1. Introduction

Rapid technological advances have aided many key innovations in remote sensing in recent years, most notably hyperspectral remote sensing. In the remote sensing world, HSRRS-image-based scene

Classification is gaining attention. Hyperspectral remote sensing has the ability to improve human perception of the earth's surface while also moving remote sensing forward. The spatial and spectral resolution of input datasets, however, determine the scale and accuracy of thematic maps. Because a picture's spatial and spectral resolutions are theoretically linked, one may be improved at the expense of the other. The extraction of scene-level discriminative characteristics is a vital step in scene classification since it bridges the large gap between an original picture and its semantic category. Researchers have developed a number of feature extraction techniques in recent years, which can be classified into three types: low-level methods, mid-level methods, and high-level methods. To deal with the spectral-spatial backdrop, deep learning techniques for HSI classification primarily focus on spectral-spatial background modelling [2][5][7][10].

This paper illustrates how to use machine learning and deep learning methods to quickly detect spatial and spectral features and extract them to enhance the classification accuracy of the HSI image dataset, which is available in spectral band and spectral image formats. One of the most important aspects of this research is how the classification accuracy varies when the two methods are combined. The main contribution of proposed system are:

- Novel hybrid neural network approach using Pretrained 3D GSHT- ConvNet - MLPNNet feature extraction and classification framework.
- Analyzing the impact of hybrid neural network approach on proposed hybrid approach.
- Unified framework that can efficiently classify both hyperspectral data, i.e. spectral band and spectral image.

The following is a breakdown of the structure of the paper. The related works are introduced and examined in section II then introduces the proposed methodology approach in section III. In Section IV, we'll look at and discuss an experimental implementation. Finally, Section V concludes this investigation and gives some reflections on the work.

2. Related Work

Based on the application of previous work, the primary classification techniques have been divided into handcrafted and automated characteristics in order to leverage second distinct statistics, which are further discussed in the next two paragraphs.

Based on the application of previous work, the basic categorization algorithms have been divided into handcrafted and automated features in order to leverage second different statistics, which are further addressed. A new supervised classification method proposed [1] based on second-order statistics computed from a deep neural network's output. The efficacy of three advanced classifiers, SAM, ANN, and SVM, assessed [2] in improving land use/land cover categorization using hyperspectral data. The use of Principal Component Analysis, Linear Discriminant Analysis, and a combination of the two are used to categorise HSI pictures [3]. The impact of dimension reduction on hyperspectral data classification systems is investigated [4]. A CTFCNN architecture developed [5] to properly utilise a pre-trained CaffeNet' s discriminant capability. To categorise the pixels of hyperspectral images, CNNs used [6] as an end-to-end pixelwise method. For remote sensing scene classification, a new lightweight remote sensing image categorization algorithm called Pruning Filter with Attention Mechanism proposed [7]. For enhanced modelling, an end-to-end architecture presented [8] for conducting band-specific spectral-spatial feature learning using a neural network. A simple and efficient complete convolutional network suggested [9] based on DenseNet as a classification method based on spatial and spectral data correlations.

The LBP 1D-CNN model is suggested [10] for HSI classification. A one-class ensemble employing SVM and KNN developed [11] based self-training algorithms for semi-supervised categorization of HSI data. A strategy that combines convolutional layer feature extraction developed [12] with ASMLR classification performance. A multi-size picture training approach suggested [13] based on a network training strategy. A Multiscale and Multiangle convolutional neural network (MSMA-CNN), introduced [14] which extracts deep information from RS pictures using several discriminants, nonlinear, and invariant convolutional, pooling, and fully connected layers. A Neural Network introduced [14] to examine how to classify hyperspectral images. A novel SVM-based classification strategy was introduced [16]. A multi-scale local binary patterns features and Fisher vectors-based image representation technique introduced [14] for remote sensing image scene classification. The performance of common aerial scene categorization and deep learning methods on AID, compared [18] which might be used as a benchmark. A model suggested [19] based on the rotational invariant local binary pattern method and a one-dimensional convolutional network (1D-CNN) applied across the histograms.

3. Proposed Methodology

A pretrained 3D ConvNet-based feature extraction framework with machine learning classifier is proposed to extract the discriminating information in hyperspectral images to improve classification performance. The pretrained 3D ConvNet technique captures two types of features from fully connected layers using a pre-trained Inception V3 and VGG16 networks with/without feature reduction techniques using ICA. Furthermore, machine learning classification operations employing two classifiers, Support Vector Machine Network (SVMNet) and Multi-Layer Perceptron Neural Network (MLPNNet) with Grid Search Hyper-tuning, are employed to get an effective prediction of Grid Search Hyper-tuning (GSHT). The block diagram of the proposed framework is shown in Figure 1.

3.1 Hyperspectral Dataset, Dataset Splitting

The hyperspectral dataset, which can be found in the Live Aerial Image Hyperspectral Dataset, is made up of spectral pictures, which are two-dimensional vectors of pixels in picture format. The framework's implementation is divided into two phases: training and testing, with the dataset requiring a 70-30 percent split in the number of samples for this process.

3.2 Feature Engineering

Feature engineering is the pre-processing step of machine learning, which extracts features from raw data. Pre-processing for the spectral band include extracting pixels and ground truth data from raw

Figure 1: Proposed framework for HSI classification

data, as well as scaling, or picture resizing, for the spectral image. In feature extraction, feature fusion of two pretrained 3D Conv Net models, inception V3 and VGG 16, is used. Figure 2 shows a detailed diagram of the Inception V3 and VGG 16 network layer design. There are four levels to this model: input, feature, classification, and output. This fusion layer is used to generate the input and feature layers, with the feature layer supplying low to high level features that define the input's spatial and spectral qualities, arranged in a hierarchy from low to high level features. Low-level features include edges and blobs, whereas high-level features include objects and events. Low-level feature extraction is done with signal/image processing techniques, whereas high-level feature extraction is done with machine learning approaches. Picture details such as lines or dots that can be recognised using a convolutional filter (for genuinely low-level stuff), SIFT, or HOG, for example, are examples of low-level features (for more abstract things like edges). High-level characteristics are placed on top of low-level features to recognise objects and larger shapes in the image. Convolutional neural networks incorporate both types of features: the first few of layers generate filters for finding lines, dots, curves, and other objects, while the latter layers learn to recognise common objects and patterns. They're so low-level because they respond to edges/gradients and corners, which are both low-level visual processing features. Using ICA, features are optimised or lowered after being extracted from these layers. ICA is an abbreviation for Independent Components Analysis. ICA is a technique for partitioning a dataset into columns of independent components in order to reduce its size. It posits that each data sample is made up of a number of independent components, and it seeks to identify these components.

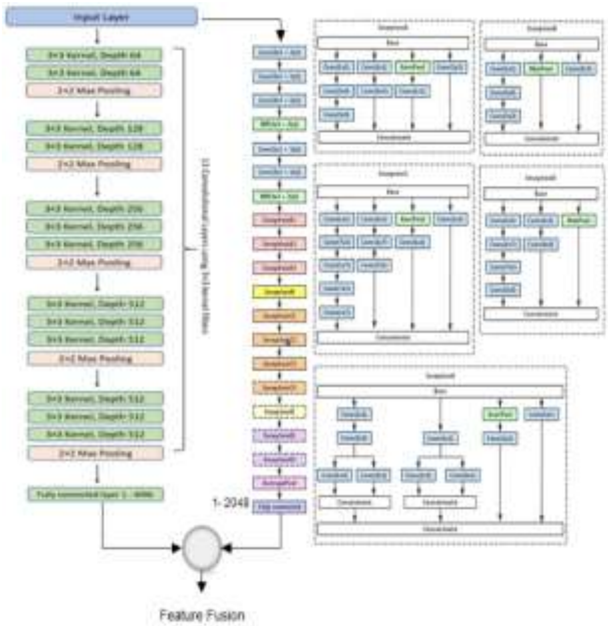

Figure 2: Architecture of Feature Fusion Layer

3.3 Model Learning, Validation, Evaluation

In classification, the GSHT-SVMNet and GSHT-MLPNNet networks are utilised, with the GSHT principle being applied to obtain maximum accuracy with K-fold validation, i.e. K=10. The process of fine-tuning hyperparameters to discover the optimum values for a given model is known as grid search. Because the hyper parameter values given impact the model's overall performance, this is critical. The trained model predicts the output label for the provided dataset after successful validation. Below is the recommended framework implementation algorithm.

Given a set of training samples with x1,...xn as fused features of HSI data and y1,y2,....yn as ground truth label HSI data

(x1, y1) (x2, y2), ...(xn, yn)

Where,

$X_i \in R^n$ and $y_i \in \{0,1\}$

$f(x) = W_2 \; g(W_1^T x + b_1) + b_2$

Where,

$W_1 \in R^m$

W_2, b_1, $b_2 \in R$ are model parameters

W_1 and W_2 are weights of input layer and hidden layer

b_1, b_2 represent the bias added to the hidden layer and the output layer respectively

g(.) : R -> R is this activation function set by hyperbolic tan

$$g(z) = \frac{e^z - e^{-z}}{e^z + e^z}$$

for binary classification f(x) passes through the logistic function

If there are more than two classes, f(x) will be of vector size (in_class).

It passes through softmax function which is

$$\text{Softmax}(z_i) = \frac{\exp(zi)}{\sum_{l=1}^{k} \exp(zi)}$$

Where,

z_i: the ith element of the input of the softmax

In gradient descent,

$$W^{i+1} = W^i - \epsilon \nabla Loss_W^i$$

Where,

i : iteration step

ϵ : learning rate

3.4 Algorithm

Algorithm Steps:

Input:

Training and Testing instance set S, a vector of feature values and the class i.e. label value

Feature Set, $F(i) = \{f_1(i), f_2(i), f_3(i), \ldots \ldots, f_1(i)\}$

Hyperspectral dataset expressed as, $X = [X_{1,}X_{2,}X_{3,}, \ldots \ldots \ldots \ldots . X_{L,}]^T \in R^{L(M \times N)} \ldots \ldots \ldots ..(i)$

where,

X: Hyperspectral input dataset

L: Number of bands / Number of images per class

M x N: Number of samples in each band

R: Hyperspectral output class

Label Set, L(i) = {Spectral Band Classes and Spectral Image Label}

Initialization:

Collect and Prepare feature data and label data from raw dataset values from Spectral Band and Spectral Image Dataset.

Feature Engineering Phase:

For each feature data

Calculate the normalized value of all features set. Scale the all-feature data into specific range.

Parameter Hyper tuning Phase

Define the model for ML Classifiers.

Define the range of possible value for all hyperparameters of ML algorithms.

Sampling of hyper parameters values using Grid Search CV Function.

Evaluate and find the best score among all hyper parameters value.

Validate the model using K-Fold Validation Learning Method.

Feature set: $F_{fused} = \{f_1, f_2\} = f(X) \ldots \ldots \ldots \ldots \ldots \ldots \ldots \ldots (ii)$

Where,

f1 : features obtained by VGG16 network

f2: features obtained by Inception V3 network

$$F_{optimized} = ICA\ (F_{fused}) \ldots \ldots \ldots \ldots \ldots \ldots \ldots (iii)$$

$$\left\{\frac{f_1}{f_2}\right\} \in S(i,j) \ldots \ldots \ldots \ldots \ldots \ldots \ldots \ldots \ldots \ldots \ldots \ldots (iv)$$

$$S(i,j) = \sum_m \sum_n (m,n)k(i-m, j-m) \ldots \ldots (v)$$

ReLu and Pooling layer:

Classifier:

$C_F = \text{Classifier}\ (F_{fused}) \dots \dots \dots \dots \dots (vi)$

Training Phase:

Initialize the parameter tuned for ML model of ML Classifiers.

Initialize the feature data and label data for training dataset.

Train the model for respective ML algorithms.

. Validate the model performance using K-fold cross validation method.

. If validation successful then save the trained model TMrf, TMmlp and if not the repeat from step 8.

Testing Phase:

. Initialize the feature data for testing dataset.

. Load the trained model of ML algorithms.

. Predict the results whether its Spectral Band Class and Spectral Image Label.

. Plot Confusion matrix between Actual Label Data and Predicted Label Data to check system accuracy.

Evaluation Phase:

. Evaluate performance of classification model C, Confusion Matrix Parameters based TP, FP, TN and FN, Accuracy, Kappa Score and MCC.

4. Experimental Results And Discussion

Dataset Description

Spectral Band Dataset (IP and UP)

There are two spectral band dataset used in this project. Indian Pines (IP) and University of Pavia (UP). The Indian Pines scene contains two-thirds agriculture, and one-third forest or other natural perennial vegetation. There are two major dual lane highways, a rail line, as well as some low-density housing, other built structures, and smaller roads. This scene was gathered by AVIRIS sensor over the Indian Pines test site in North-western Indiana and consists of 145\times145 pixels and 224 spectral reflectance bands in the wavelength range 0.4–2.5 10^(-6) meters. The ground truth available is designated into sixteen classes and is not all mutually exclusive. In University of Pavia, these is the scene acquired by the ROSIS sensor during a flight campaign over Pavia, northern Italy. The number of spectral bands is 103 for Pavia University. Pavia University is 610*610 pixels, but some of the samples in the images contain no information and have to be discarded before the analysis. The geometric resolution is 1.3 meters. Image ground truths differentiate 9 classes each. It can be seen the discarded samples in the figures as abroad black strips.

Spectral Image Dataset (AID)

Google Earth imagery from the Mumbai and Pune subregions was used to compile the collection. The spatial resolution of the photo’ s ranges from 0.5 m to 8 m, and each scene contains 500x500 pixels. There are 700 photos in total in the collection, which are classified into seven semantic groups. The total amount of scene photographs in each class, which includes airports, beaches, forests, mountains, railway stations, rivers, and stadiums.

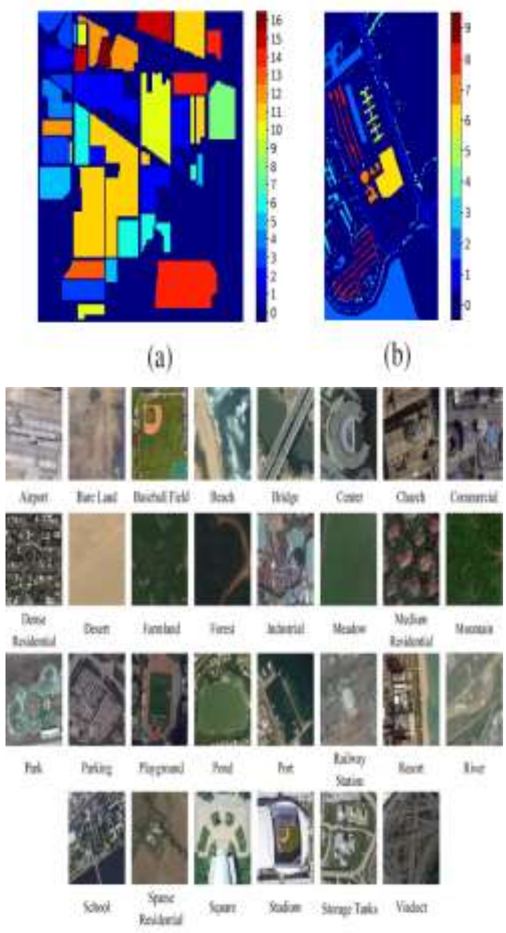

c)

Figure 3: Ground truth images of (a) Indian Pines and (b) Pavia University C) AID datasets.

4.2 Experimental Setup

All experiments were performed on a laptop equipped with 16-GB memory, i5-8500 CPU, and 64-bit Windows 10 with python as programming language. The anaconda distribution with Keras, Tensorflow and Scikit learn toolbox was employed to exact different features and classification.

4.3 Performance Analysis

The classification efficiency measure is constructed from a confusion matrix that provides the result of counting correctly and incorrectly identified cases by event class (normal / abnormal). Therefore, some statistically defined measurements are taken into account and used as the basis for comparative analysis of classifiers. There are four basic metrics used in the confusion matrix to describe performance measurements. True positive (TP). Represents the number of correct positive predictions found in the hyperspectral band or image test set. True Negatives (TN), representing a set of correct negative predictions within a hyperspectral band or image test set. False positives (FP). Represents the number of false positive predictions in the hyperspectral band or image test set. False Negative (FN), which represents the number of false negative predictions in a hyperspectral band or image test set.

$Accuracy = (TP+TN)/(TP+TN+FP+FN)$

$Precision = TP/(TP+FP)$

$Recall = TP/(TP+FN)$

$MCC = (TP*TN) – (FP*FN) / sqrt((TP+FP)(TP+FN)(TN+FP)(TN+FN))$

where, TP – true positive, TN – true negative, FP – false positive, FN – false negative

The live aerial dataset is examined related to spectral images for categorization in this experiment. The dataset is divided into two sections for training and testing. The training set contains 70% of the original data matrix, whereas the independent test set has 30%. The grid search hyperparameter optimization approach, as indicated in table 1, is employed in our experiment to optimize the parameters of the classifier model. From the confusion matrix parameters, the accuracy, precision, recall, f-score, Matthews Correlation Coefficient (MCC), and Kappa Score parameters are assessed and displayed in table 2-6. Also, comparison with existing state of art methods also described in table 7 and its representation is given in fig 4.

Table 1: Grid Search Hyperparameter for training of classifiers

Datasets	GSHT-SVM-Net (%)	GSHT-MLPNet (%)	PT-3D-GSHT-SVM-Net (%)	PT-3D-GSHT-MLPNNet (%)
University of Pavia (Spectral Band)	87	94	89	**96**
Indian Pines (Spectral Band)	79	83	80	**85**
AID (Spectral Image)	25	29	86	**89**

Table 2 depicts that accuracy is better in case of spectral band dataset using both classifiers, GSHT-SVMNet and GSHT-MLPNet than spectral image dataset. But in case of proposed PT-3D-GSHT approach using both classifier SVMNet and MLPNNet, spectral band and spectral image datasets found to be effective in term of accuracy performance due to the rich feature representation of PT-3D-Conv-Net model. Similarly, it is found that from Table 3-4, proposed PT-3D-GSHT framework is effective for all types of datasets.

Table 2: Accuracy Performance of classifiers on both datasets

Datasets	**Framework**	**Hyper-parameter tuning**
IP	PT-3D-GSHT-SVMNet	C=10, cache_size=1024, kernel='poly', probability=True
	PT-3D-GSHT-MLPNNet	alpha=1e-05, max_iter=1000, random_state=500
UP	PT-3D-GSHT-SVMNet	C=10, cache_size=1024, kernel='poly', probability=True
	PT-3D-	alpha=1e-05,

	GSHT-MLPNNet	max_iter=1000, random_state=500
AID	PT-3D-GSHT-SVMNet	activation='relu', alpha=1e-05, batch_size='auto', beta_1=0.9, beta2=0.99, epsilon=1e-08, hidden_layer_size=100, learning_rate='constant', max_fun=15000, max_iter=1000, random_state=500
	PT-3D-GSHT-MLPNNet	activation='relu', alpha=1e-05, batch_size='auto', beta_1=0.9, beta2=0.99, epsilon=1e-08, hidden_layer_size=100, learning_rate='constant', max_fun=15000, max_iter=1000, random_state=500

Table 3: Precision Performance of classifiers on both datasets

Datasets	**GSHT-SVM-Net (%)**	**GSHT-MLPNet (%)**	**PT-3D-GSHT-SVM-Net (%)**	**PT-3D-GSHT-MLPNNet (%)**
University of Pavia (Spectral Band)	89	95	92	**97**
Indian	81	84	78	**87**

Pines (Spectral Band)				
AID (Spectral Image)	27	32	88	**90**

Table 4: Recall Performance of classifiers on both datasets

Datasets	**GSHT-SVM-Net (%)**	**GSHT-MLPNet (%)**	**PT-3D-GSHT-SVM-Net (%)**	**PT-3D-GSHT-MLPNNet (%)**
University of Pavia (Spectral Band)	83	92	84	**94**
Indian Pines (Spectral Band)	75	80	76	**82**
AID (Spectral Image)	23	27	82	**87**

Similarly, as described in Table 5, kappa score is found to be much better for University of Pavia, spectral band dataset as compared to other datasets. But kappa score for proposed PT-3D-GSHT-MLPNNet classifier indicates that how closely the instances classified by the classifier matched with the data labeled as ground truth.

In table 6, MCC performance is found to be effective for two types of datasets using PT-3D-GSHT-MLPNNet as compared to PT-3D-GSHT-SVMNet. It indicates that how all the parameters of confusion matrix is effectively categorized.

Table 5: Kappa Score Performance of classifiers on both datasets

Datasets	**GSHT-SVM-Net (%)**	**GSHT-MLPNet (%)**	**PT-3D-GSHT-SVM-Net (%)**	**PT-3D-GSHT-MLPNNet (%)**
University of Pavia (Spectral Band)	86	92	88	**95**
Indian Pines (Spectral Band)	82	82	76	**86**
AID (Spectral Image)	30	34	87	**88**

Table 6: MCC Performance of classifiers on both datasets

Datasets	**GSHT-SVM-Net (%)**	**GSHT-MLPNet (%)**	**PT-3D-GSHT-SVM-Net (%)**	**PT-3D-GSHT-MLPNNet (%)**
University of Pavia (Spectral	84	93	85	**95**

Band)				
Indian Pines (Spectral Band)	76	81	78	**84**
AID (Spectral Image)	22	28	84	**88**

Table 7: Result Comparison with State of Art Techniques

Dataset	**References**	**Accuracy**
University of Pavia (Spectral Band)	OCESS [11]	0.8697
	PCA, SVM [16]	0.9102
	PT-3D-GSHT-MLPNNet (Proposed framework)	0.96
Indian Pines (Spectral Band)	PCA+LDA, SVM [3]	0.8251
	LBP, SVM [10]	0.8241
	OCESS [11]	0.7984
	PT-3D-GSHT-MLPNNet (Proposed framework)	0.85
AID (Spectral Image)	MCBGP + E-ELM [17]	0.86
	ResNet [18]	0.85
	PT-3D-GSHT-MLPNNet	0.89

	(Proposed framework)	

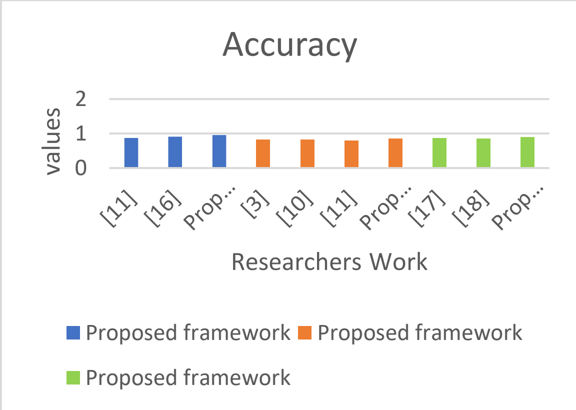

Figure 4: accuracy performance of existing state of art method

The performance of proposed method is compared to existing state-of-the-art algorithms as described in table 7. Though researchers have classified hyperspectral data using various model techniques for three datasets UP, IP and AID, it is found that the proposed framework is efficient in terms of accuracy parameters due to hybrid neural network approach in which rich information of features are extracted using PT-3D-ConvNet and classification is performed using MLPNNet.

5. Conclusion

In this paper, a hybrid neural network framework for spectral band and spectral image datasets is presented, which combines machine learning and deep learning to fully exploit the discriminant feature extraction power of a pre-trained deep neural network model as well as the classification capabilities of neural network classifier models. The feature extractor in this framework uses features from deep neural network with fusion of both pretrained models VGG16 and InceptionV3 to collect multilayer convolutional features and features from the fully connected layer. Finally, weighted concatenation is used to integrate these features. As a result, the proposed system can generate hyperspectral aerial picture representations while also improving scene categorization accuracy. Experiments performed on hyperspectral data spectral band and spectral image show that the proposed method with pretrained feature using hybrid neural network outperforms existing conventional feature methods in terms of overall accuracy, with the highest OAs achieved for University of Pavia, Indian Pine both spectral band dataset and AID, spectral Image dataset being 0.96, 0.85, and 0.89, respectively. To increase classification performance, we'll incorporate fine-tuning algorithms and focus on combining variables from diverse regions of interest (ROIs) with large dataset combining unsupervised approach in the future. Despite the proposed model's enhanced performance in the spatial-spectral domain of hyperspectral data, more research into how the technique might be improved is needed with help of deep learning. Future study will also include an analysis based on the concatenation of separate chains of pretrained CNN models.

References

1. S. Akodad, S. Vilfroy, L. Bombrun, C. C. Cavalcante, C. Germain and Y. Berthoumieu, "An ensemble learning approach for the classification of remote sensing scenes based on covariance pooling of CNN features," 2019 27th European Signal Processing Conference (EUSIPCO), 2019, pp. 1-5, doi: 10.23919/EUSIPCO.2019.8902561.
2. V. S. Sahithi, S. Subbiah and S. Agrawal, "Comparison of Support Vector Machine, Artificial Neural Networks and Spectral Angle Mapper Classifiers on Fused Hyperspectral Data for Improved LULC Classification," 2019 8th International Conference on Modeling Simulation and Applied Optimization (ICMSAO), 2019, pp. 1-6, doi: 10.1109/ICMSAO.2019.8880336.
3. A. A. Joy, M. A. M. Hasan and M. A. Hossain, "A Comparison of Supervised and Unsupervised Dimension Reduction Methods for Hyperspectral Image Classification," 2019 International Conference on Electrical, Computer and Communication Engineering (ECCE), 2019, pp. 1-6, doi: 10.1109/ECACE.2019.8679360.
4. L. Younus and N. G. Kasapoglu, "Dimension Reduction and Its Effects in Hyperspectral Data Classification," 2019 6th International Conference on Electrical and Electronics Engineering (ICEEE), 2019, pp. 359-366, doi: 10.1109/ICEEE2019.2019.00076.
5. Huang, Hong, and Kejie Xu."Combing Triple-Part Features of Convolutional Neural Networks for Scene Classification in Remote Sensing" Remote Sensing 11, 2019, no. 14: 1687. https://doi.org/10.3390/rs11141687
6. Zhong, Zilong & Li, Jonathan. “Hyperspectral image classification using deep convolutional neural networks” , 2017 Journal of Computational Vision and Imaging Systems. 3. 10.15353/vsnl.v3i1.178.
7. Zhang, Shuo, Gengshen Wu, Junhua Gu, and Jungong Han. "Pruning Convolutional Neural Networks with an Attention Mechanism for Remote Sensing Image Classification", 2020 Electronics 9, no. 8: 1209. https://doi.org/10.3390/electronics9081209

8. Bidari, S. Chickerur, H. Ranmale, S. Talawar, H. Ramadurg and R. Talikoti, "Hyperspectral Imagery Classification Using Deep Learning," 2020 Fourth World Conference on Smart Trends in Systems, Security and Sustainability (WorldS4), 2020, pp. 672-676, doi: 10.1109/WorldS450073.2020.9210332.
9. Zhang, Jianming & Lu, Chaoquan & Li, Xudong & Kim, Hye-Jin & Wang, Jin., "A full convolutional network based on DenseNet for remote sensing scene classification" , 2019 Mathematical Biosciences and Engineering. 16. 3345-3367. 10.3934/mbe.2019167.
10. A. V. Miclea, R. Terebes and S. Meza, "One dimensional convolutional neural networks and local binary patterns for hyperspectral image classification," 2020 IEEE International Conference on Automation, Quality and Testing, Robotics (AQTR), 2020, pp. 1-6, doi: 10.1109/AQTR49680.2020.9129920.
11. P. S. Singh, V. P. Singh, M. K. Pandey and S. Karthikeyan, "One-class Classifier Ensemble based Enhanced Semisupervised Classification of Hyperspectral Remote Sensing Images," 2020 International Conference on Emerging Smart Computing and Informatics (ESCI), 2020, pp. 22-27, doi: 10.1109/ESCI48226.2020.9167650.
12. S. Kutluk, K. Kayabol and A. Akan, "Spectral-Spatial Classification of Hyperspectral Images Using CNNs and Approximate Sparse Multinomial Logistic Regression," 2019 27th European Signal Processing Conference (EUSIPCO), 2019, pp. 1-5, doi: 10.23919/EUSIPCO.2019.8902983.
13. Zhang, Jianming, Chaoquan Lu, Jin Wang, Xiao-Guang Yue, Se-Jung Lim, Zafer Al-Makhadmeh, and Amr Tolba, "Training Convolutional Neural Networks with Multi-Size Images and Triplet Loss for Remote Sensing Scene Classification", 2020 Sensors 20, no. 4: 1188. https://doi.org/10.3390/s20041188
14. Alegavi, S.S. & Sedamkar, R.R. "Implementation of deep convolutional neural network for classification of multiscaled and multiangled remote sensing scene" , 2020 Intelligent Decision Technologies. 14. 1-14. 10.3233/IDT-190076.
15. T. Singh and T. Babu, "Fractal Image Processing and Analysis for Classification of Hyperspectral Images," 2019 10th International Conference on Computing, Communication and Networking Technologies (ICCCNT), 2019, pp. 1-6, doi: 10.1109/ICCCNT45670.2019.8944410.
16. D. K. Pathak and S. K. Kalita, "Spectral Spatial Feature Based Classification of Hyperspectral Image Using Support Vector Machine," 2019 6th International Conference on Signal Processing and Integrated Networks (SPIN), 2019, pp. 430-435, doi: 10.1109/SPIN.2019.8711731.

17. Huang, Longhui, Chen Chen, Wei Li, and Qian Du, "Remote Sensing Image Scene Classification Using Multi-Scale Completed Local Binary Patterns and Fisher Vectors", 2016, Remote Sensing 8, no. 6: 483. https://doi.org/10.3390/rs8060483
18. G. Xia et al., "AID: A Benchmark Data Set for Performance Evaluation of Aerial Scene Classification," in IEEE Transactions on Geoscience and Remote Sensing, vol. 55, no. 7, pp. 3965-3981, July 2017, doi: 10.1109/TGRS.2017.2685945.
19. A. V. Miclea, R. Terebes and S. Meza, "One dimensional convolutional neural networks and local binary patterns for hyperspectral image classification," 2020 IEEE International Conference on Automation, Quality and Testing, Robotics (AQTR), 2020, pp. 1-6, doi: 10.1109/AQTR49680.2020.9129920
20. https://in.mathworks.com/help/deeplearning/ug/pretrained-convolutional-neural-networks.html
21. X. Cao, J. Yao, Z. Xu and D. Meng, "Hyperspectral Image Classification With Convolutional Neural Network and Active Learning," in IEEE Transactions on Geoscience and Remote Sensing, vol. 58, no. 7, pp. 4604-4616, July 2020, doi: 10.1109/TGRS.2020.2964627.
22. X. Yang, Y. Ye, X. Li, R. Y. K. Lau, X. Zhang and X. Huang, "Hyperspectral Image Classification With Deep Learning Models," in IEEE Transactions on Geoscience and Remote Sensing, vol. 56, no. 9, pp. 5408-5423, Sept. 2018, doi: 10.1109/TGRS.2018.2815613.